Journal of Engineering Physics and Thermophysics, Vol. 75, No. 4, 2002

NUMERICAL MODELING OF HEAT AND MASS TRANSFER IN A LOW-TEMPERATURE HEAT PIPE

G. V. Kuznetzov and A. E. Sitnikov

UDC 536.24

A mathematical model of heat and mass transfer in a low-temperature heat pipe has been formulated. Numerical modeling of the problem of heat and mass transfer has been carried out. The distributions of the velocities, the pressure, and the temperatures in the heat pipe have been obtained. The results can be employed in analyzing the efficiency and power of low-temperature heat pipes.

Low-temperature heat pipes are one of the most promising basic elements of the systems that provide the thermal regime in spacecraft of the type of communications and broadcasting satellites [1]. The characteristics of heat pipes are predicted at present predominantly on the basis of generalization of experimental data on the intensity of heat transfer [2]. But the empirical base can be incomplete in many cases and makes it impossible to predict the parameters of heat pipes for a wide range of variation of their operating conditions [1]. Rather many works devoted mainly to experimental investigations of the regularities of heat and mass transfer in heat pipes (for example, [2, 3]) have been published to date. The general mathematical model of these processes formulated rather long ago [4] has not been realized completely at present.

The present investigation seeks to mathematically model heat and mass transfer in low-temperature heat pipes for steady-state operating regimes with allowance for the local heat release along the external contour of the pipes.

Physical Model. We consider the problem on the temperature field in a hollow metal cylinder over the interior surface of which a liquid cooling agent moves under the action of the surface-tension forces. A heat flux of prescribed intensity which is caused by the heat release of a unit of radioelectronic equipment or other heat source is acting on a portion of the external boundary of a cylinder of finite dimensions. In the cooling-agent zone adjacent to the portion of heat release, the temperature increases to a value for which the cooling agent begins to evaporate. The absorption of heat expended on the phase transition of the liquid cooling agent to a vapor occurs. The products of evaporation move from the phase interface to the axis of symmetry of the cylinder. The difference of the vapor pressure along the longitudinal coordinate z is formed. Under the action of this pressure gradient, the vapor of the cooling agent moves from the zone of high pressure (and relatively high temperatures) to a zone of low pressure (and relatively low temperatures). Condensation of the vapor of the cooling agent occurs in the region of temperatures decreased as compared to the region of maximum temperatures; heat is released. The condensate resulting from the phase transition is spreading over the tube portion whose boundaries are determined by the thermodynamic parameters of the process [4]. The liquid cooling agent fills a capillary structure, which covers the entire interior surface of the cylinder, in the condensate zone. The liquid cooling agent, under the action of the surface-tension forces, moves in capillaries from the condensation zone to the evaporation zone. As a result of circulatory motion the energy from the region where the radioelectronic equipment is located is transferred to the region of relatively low temperatures [1]. A simplified scheme of the process of heat transfer is presented in Fig. 1.

The problem is considered under the following basic assumptions:

(1) the distribution of the magnitude of the external flow along the circular coordinate is not taken into account; solution is carried out in an axisymmetric formulation;

(2) the wick represents a layer of a cooling agent; the motion of the condensate is described by Darcy's law [4];

(3) the motion of the vapor is described within the framework of the Prandtl model for the boundary layer;

Scientific-Research Institute of Applied Mathematics and Mechanics at Tomsk State University, Tomsk, Russia. Translated from Inzhenerno-Fizicheskii Zhurnal, Vol. 75, No. 4, pp. 58–64, July–August, 2002. Original article submitted July 31, 2001; revision submitted January 11, 2002.

 1062-0125/02/7504-0840$27.00

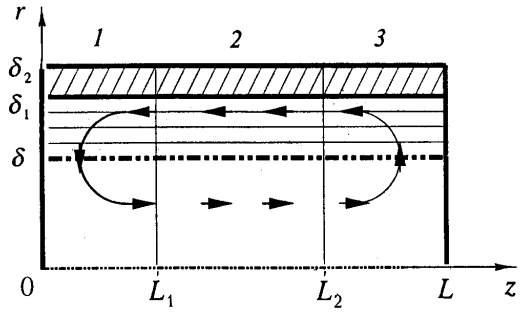

Fig. 1. Scheme of the process of heat transfer ($\delta_1 \le r \le \delta_2$, casing of the heat pipe; $\delta \le r \le \delta_1$, liquid phase; $0 \le r \le \delta$, vapor phase): 1) evaporation zone; 2) transport zone; 3) condensation zone. r, z, m.

(4) the processes of heat and mass transfer are steady-state;

(5) the coefficients of transfer (thermal conductivity, viscosity) are independent of temperature;

(6) the exterior surface is heat-insulated for $L_1 < z < L_2$ except for the following portions: (a) $0 < z < L_1$ (heat source) and (b) $L_2 < z < L$ (zone of heat removal by radiation);

(7) contacts at the interphase boundaries and at the "casing of the heat pipe — condensate" boundary are considered to be ideal;

(8) mass forces are absent;

(9) radiative heat exchange can be disregarded;

(10) the state of boiling of the cooling agent is not reached.

Mathematical Model. The system of equations which describe heat and mass transfer in a cylindrical coordinate system with an axis of symmetry coincident with the axis of symmetry of the heat pipes involves the equations of conservation of mass, momentum, and energy for the liquid and vapor phases of the cooling agent and the heat-conduction equation for the casing of the heat pipe. The hydrodynamic and thermal problems for the vapor phase of the cooling agent have been solved within the framework of the model of a laminar boundary layer [5]:

$$0 \le z \le L, \quad \delta_1 \le r \le \delta_2: \quad \left(\frac{\partial^2 T_1}{\partial r^2} + \frac{1}{r} \frac{\partial T_1}{\partial r} + \frac{\partial^2 T_1}{\partial z^2} \right) = 0, \tag{1}$$

$$r = \delta_2: \quad \lambda_1 \left. \frac{\partial T_1}{\partial r} \right|_{0<z\le L_1} = q, \tag{2}$$

$$r = \delta_2: \quad \lambda_1 \left. \frac{\partial T_1}{\partial r} \right|_{L_1<z\le L_2} = 0, \tag{3}$$

$$r = \delta_2: \quad \lambda_1 \left. \frac{\partial T_1}{\partial r} \right|_{L_2<z\le L} = \sigma_1 \varepsilon T_{\text{surf}}^4, \tag{4}$$

$$z = 0: \quad \lambda_1 \left. \frac{\partial T_1}{\partial z} \right|_{\delta_1\le r\le\delta_2} = 0, \tag{5}$$

$$z = L: \qquad \lambda_1 \left.\frac{\partial T_1}{\partial z}\right|_{\delta_1 \le r \le \delta_2} = 0\,, \tag{6}$$

$$r = \delta_1: \qquad \lambda_1 \left.\frac{\partial T_1}{\partial r}\right|_{0<z\le L} = \lambda_2 \left.\frac{\partial T_2}{\partial r}\right|_{0<z\le L}, \quad T_1 = T_2\,, \tag{7}$$

$$0 \le z \le L\,, \quad \delta \le r \le \delta_1: \quad \begin{cases} \dfrac{\partial P_2}{\partial z} = \dfrac{\partial P_3}{\partial z} - 2\sigma \dfrac{\partial}{\partial z}\left(\dfrac{1}{R_{\text{curv}}(z)}\right), & (8) \\ u_2 = -\dfrac{K}{\mu_2 \varepsilon_1}\dfrac{\partial P_2}{\partial z}\,, & (9) \\ C_2 \rho_2 \left(u_2 \dfrac{\partial T_2}{\partial z}\right) = \lambda_2 \left(\dfrac{\partial^2 T_2}{\partial r^2} + \dfrac{1}{r}\dfrac{\partial T_2}{\partial r} + \dfrac{\partial^2 T_2}{\partial z^2}\right), & (10) \end{cases}$$

$$z = 0: \qquad u_2(r, z)\big|_{\delta<r<\delta_1} = 0\,, \tag{11}$$

$$z = 0: \qquad \lambda_2 \left.\frac{\partial T_2}{\partial z}\right|_{\delta \le r<\delta_1} = 0\,, \tag{12}$$

$$z = L: \qquad \lambda_2 \left.\frac{\partial T_2}{\partial z}\right|_{\delta \le r<\delta_1} = 0\,, \tag{13}$$

$$r = \delta: \qquad \lambda_2 \left.\frac{\partial T_2}{\partial r}\right|_{0<z\le L_1} = \lambda_3 \left.\frac{\partial T_3}{\partial r}\right|_{0<z\le L_1} - W_1 Q\,, \quad T_2 = T_3\,, \tag{14}$$

$$r = \delta: \qquad \lambda_2 \left.\frac{\partial T_2}{\partial r}\right|_{L_2<z\le L} = \lambda_3 \left.\frac{\partial T_3}{\partial r}\right|_{L_2<z\le L} + W_2 Q\,, \quad T_2 = T_3\,, \tag{15}$$

$$r = \delta_1: \qquad \lambda_1 \left.\frac{\partial T_1}{\partial r}\right|_{0<z\le L} = \lambda_2 \left.\frac{\partial T_2}{\partial r}\right|_{0<z\le L}, \quad T_1 = T_2\,, \tag{16}$$

$$r = \delta: \qquad \lambda_2 \left.\frac{\partial T_2}{\partial r}\right|_{L_1<z\le L_2} = \lambda_3 \left.\frac{\partial T_3}{\partial r}\right|_{L_1<z\le L_2}, \quad T_2 = T_3\,, \tag{17}$$

$$0 \le z \le L, \quad 0 \le r \le \delta: \quad \begin{cases} \rho_3 u_3 \dfrac{\partial u_3}{\partial z} + \rho_3 v_3 \dfrac{\partial u_3}{\partial r} = -\dfrac{dP_3}{dz} + \mu_3 \left(\dfrac{1}{r} \dfrac{\partial u_3}{\partial r} + \dfrac{\partial^2 u_3}{\partial r^2} \right), & (18) \\ \dfrac{\partial (u_3 \rho_3 r)}{\partial z} + \dfrac{\partial (v_3 \rho_3 r)}{\partial r} = 0, & (19) \\ C_3 \rho_3 \left(u_3 \dfrac{\partial T_3}{\partial z} + v_3 \dfrac{\partial T_3}{\partial r} \right) = \lambda_3 \left(\dfrac{\partial^2 T_3}{\partial z^2} + \dfrac{1}{r} \dfrac{\partial T_3}{\partial r} + \dfrac{\partial^2 T_3}{\partial r^2} \right), & (20) \\ \rho_3 = \dfrac{P_3 M}{R_1 T_3}, & (21) \end{cases}$$

$$z = 0: \quad u_3 (r, z)\big|_{0<r<\delta} = 0, \tag{22}$$

$$0 \le z \le L: \quad \left.\frac{\partial u_3}{\partial r}\right|_{r \to 0} = 0, \tag{23}$$

$$r = \delta: \quad u_3 (r, z)\big|_{0<z<L} = 0, \tag{24}$$

$$r = 0: \quad v_3 (r, z)\big|_{0<z<L} = 0, \tag{25}$$

$$r = 0: \quad \lambda_3 \left.\frac{\partial T_3}{\partial r}\right|_{0 \le z \le L} = 0, \tag{26}$$

$$r = \delta: \quad \lambda_2 \left.\frac{\partial T_2}{\partial r}\right|_{L_1<z\le L_2} = \lambda_3 \left.\frac{\partial T_3}{\partial r}\right|_{L_1<z\le L_2}, \quad T_2 = T_3, \tag{27}$$

$$z = 0: \quad \lambda_3 \left.\frac{\partial T_3}{\partial z}\right|_{0 \le r \le \delta} = 0, \tag{28}$$

$$z = L: \quad \lambda_3 \left.\frac{\partial T_3}{\partial z}\right|_{0 \le r < \delta} = 0. \tag{29}$$

The mass velocity of evaporation has been calculated from the formula [4]

$$W_1 = \frac{A (P - P^{\text{sat}})}{\sqrt{2\pi R_1 T_{\text{ph.b}}/M}}. \tag{30}$$

Unlike the boundary-layer problems for external flow in the case of channel motion, the prescribed quantity is the rate of flow of the liquid through the cross section rather than the pressure.

Methods Employed. The problem has been solved by the finite-difference method [6]. The one-dimensional equations were solved using the iteration method and the implicit four-point difference scheme [5]. In the first itera-

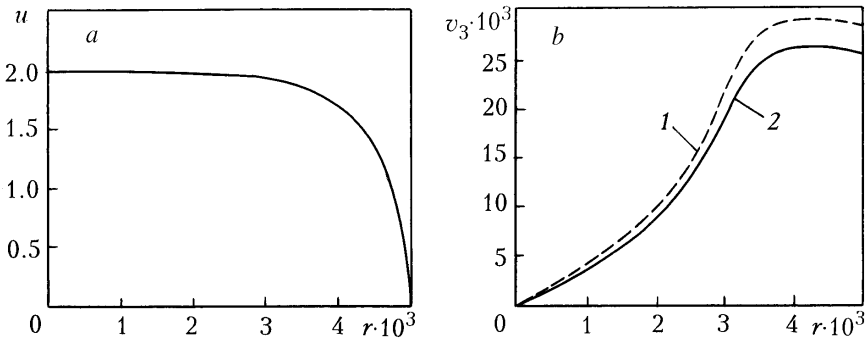

Fig. 2. Distributions of the longitudinal (a) and radial (b) components of the velocity over r for $z = 0.1$ m: 1) experiment; 2) calculation. u and v, m/sec; r, m.

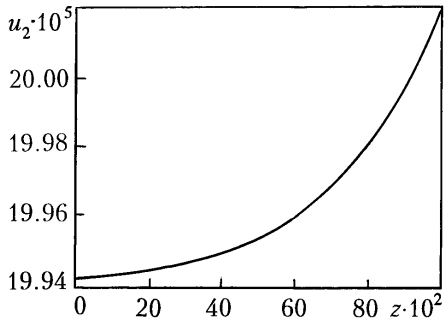

Fig. 3. Distribution of the longitudinal component of the velocity in the liquid phase for $r = 6 \cdot 10^{-3}$ m. u, m/sec; r, m.

tion, in obtaining the marching coefficients in forward marching, the values of the longitudinal $u_m^{n+1/2}$ and transverse $v_m^{n+1/2}$ velocities were set equal to the values of u_m^n and v_m^n respectively; thereafter the values of u_m^{n+1} were computed in backward marching, where $n = 0, ..., N$ and $m = 0, ..., M$. The first iteration (as all the subsequent ones) ended with computation of $v_m^{n+1/2}$. The second and all the subsequent iterations began with obtaining the marching coefficients, in computing which we employed the values of u_m^{n+1} and $v_m^{n+1/2}$ obtained in the previous iteration. Upon calculating the marching coefficients, we computed new values of u_m^{n+1} and simultaneously the maximum of the modulus of the difference between the values of u_m^{n+1} in this iteration and the previous one:

$$\Delta u^* = \max \left| \Delta u_m \right| , \quad m = 1, 2, ... ,$$

which characterizes the convergence of iterations for u. The iterations were completed when Δu^* attained a value lower than the positive number ε^* [5]. The pressure of the saturated vapor was calculated by the Ridel–Planck–Miller method [7].

The difference analogs of the differential equations of energy balance have been solved by the subincremental method (method of fractional steps) [5, 8] and by the establishment method. We calculate the transfer of heat over z at the first step and over r at the second step with the use of one-dimensional difference equations.

Analysis of Results and Discussion. In the numerical calculations, we employed thermophysical characteristics for the casing of the heat pipe made of aluminum alloy and the working fluid NH_3 (for the liquid and vapor phases) [7, 9].

Figure 2 shows the distributions of the longitudinal and radial components of the velocity in the vapor phase. The maximum of the radial-velocity component is located near the interface of the media (liquid–vapor). This is caused by the evaporation of the liquid cooling agent at the boundary of two media (liquid–vapor). As the pipe axis is approached, the radial-velocity component decreases to zero. Figure 2b gives the calculated and experimental data on this component of the velocity which have been obtained under conditions corresponding to calculation. As is seen

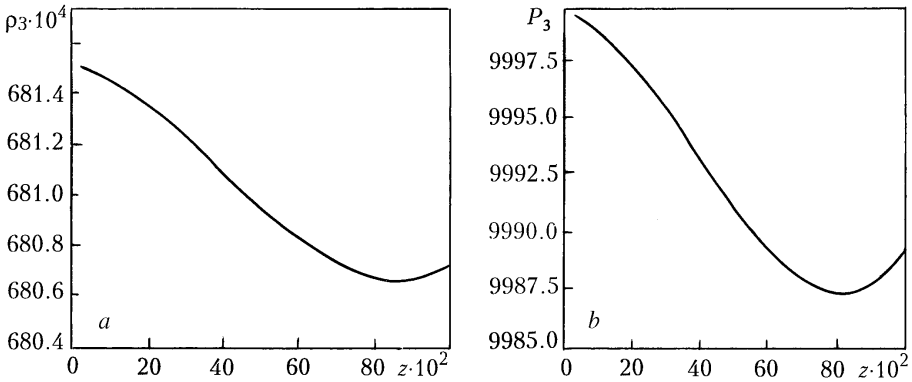

Fig. 4. Density (a) and pressure (b) distributions along the heat pipe for $r = 3 \cdot 10^{-3}$ m. ρ, kg/m^3; P, N/m^2; z, m.

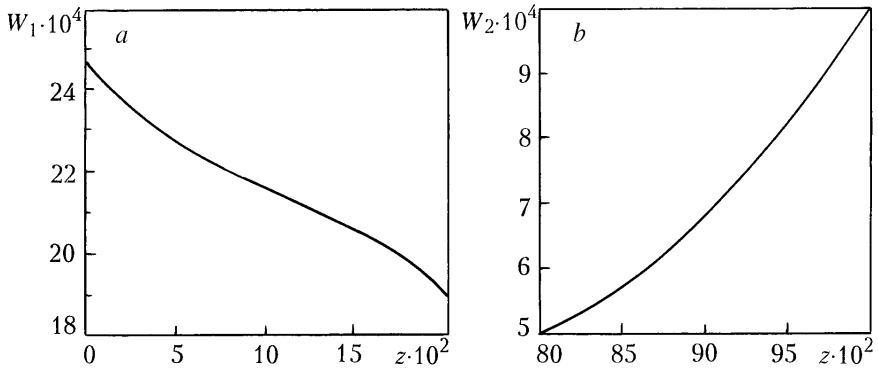

Fig. 5. Distributions of the mass velocity of evaporation (a) and condensation (b) of a cooling agent over z for $r = 3 \cdot 10^{-3}$ m. W, kg/(m^2·sec); z, m.

in the figure, the calculations yield a satisfactory coincidence with the data of the experiment [2, 4, 10]. Their disagreement is no higher than 35%.

Figure 3 shows the distribution of the longitudinal component of the velocity in the liquid phase over the coordinate z.

The distributions of the density and the pressure of the vapor over the heat-pipe length are given in Fig. 4. As is seen in Fig. 4b, the pressure decreases just to the condensation zone; thereafter it increases insignificantly due to the retardation of vapor molecules at the pipe end, because of which the density of the vapor in the condensation zone increases somewhat. Comparing the results of the numerical analysis to the experimental data on distribution of the vapor pressure [4, 10] under the equivalent conditions, we can infer that the derivations of the calculated dependence from experiment are insignificant (no higher than 30%).

The mass velocity of evaporation and condensation of the cooling agent is given in Fig. 5. A decrease in the mass velocity of evaporation is a consequence of the decrease in the vapor temperature over the pipe length. Analogously, we can infer that as the temperature of the vapor in the condensation zone increases the mass velocity of condensation increases.

Figure 6 shows the temperature distributions over the radius of the heat pipe in the zones of evaporation and condensation for different densities of the heat flux. As is seen in the figures, significant temperature gradients occur in small regions near the boundaries of the media (casing of the heat pipe–liquid and liquid–vapor). This is caused by the absorption (release) of heat in phase transitions and by the change in the thermophysical parameters of the medium in crossing these boundaries.

Figure 7 shows the distributions of the vapor temperatures along the heat pipe for a heat-flux density of 100 and 60 W/m^2. As is seen in the figure, the temperature difference over the pipe length is no higher than 2 K.

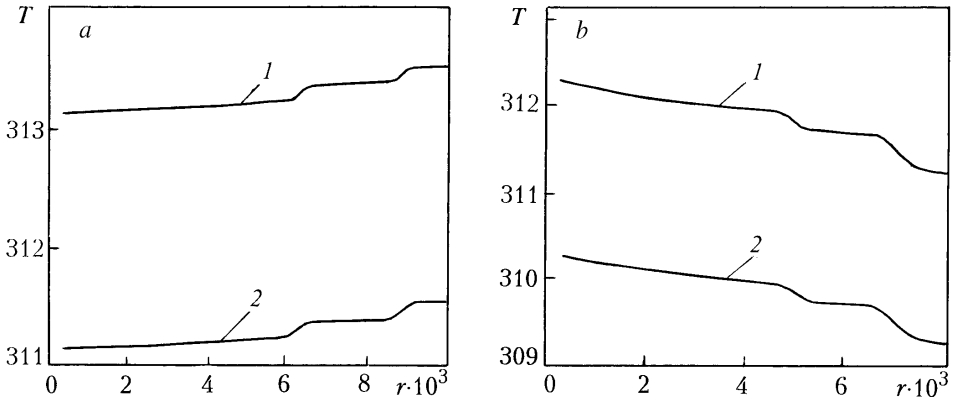

Fig. 6. Temperature distributions over the radius of the heat pipe in the evaporation zone for $z = 0.1$ m (a) and in the condensation zone for $z = 0.9$ m (b): 1) $q = 100$ and 2) 60 W/m^2. T, K; r, m.

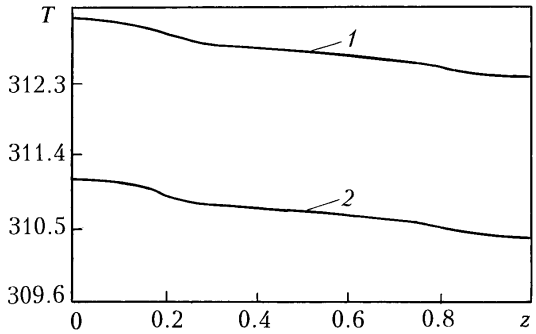

Fig. 7. Distributions of the vapor temperature along the heat pipe for $r = 3\cdot10^{-3}$ m: 1) $q = 100$ and 2) 60 W/m^2. T, K; z, m.

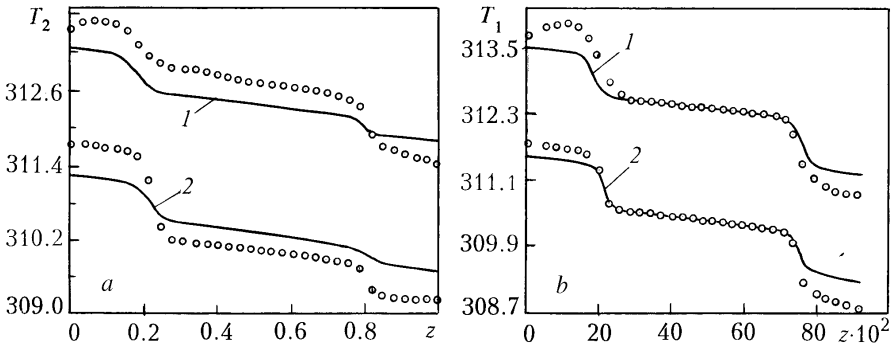

Fig. 8. Temperature distributions along the heat pipe for the liquid phase for $r = 6\cdot10^{-3}$ m (a) and over the casing of the heat pipe for $r = 8\cdot10^{-3}$ m (b): 1) $q = 100$ and 2) 60 W/m^2; points, experiment; curves, calculation. T, K; z, m.

The typical temperature distributions along the heat pipe for the liquid phase and the casing of the heat pipe are shown in Fig. 8. The comparison of the results of numerical modeling of the process and the experimental data [4, 10] has shown that numerical calculations yields a satisfactory agreement with the experiments.

In closing, it should be noted that the mathematical model of heat and mass transfer in low-temperature heat pipes which is presented in this work is based on the physical model of operation of heat pipes formulated rather long ago [2, 4] and allowing for a combination of basic processes of heat and mass transfer in the solid (casing), liquid, and vapor phases of the heat pipe. To implement this mathematical model one needs only empirical constants which can be determined under ordinary laboratory conditions (for example, the viscosity of the cooling agent and the per-

meability of the wick), have been known rather long ago (thermal effects of phase transitions), or can be calculated according to the existing procedures (thermophysical characteristics of the vapor phase). Special experiments with scale models of the heat pipes under study are not necessary for a numerical analysis on the basis of the mathematical model proposed.

In this work, we have considered the structural scheme of a heat pipe which does not allow for certain additional elements characteristic of the actual structures of heat exchangers based on heat pipes [1, 2]. Such elements can include, for example, adhesive joints between the heat pipe and the radioelectronic device, or the heat pipe and the panel on which sources of heat release are located [2], or the heat pipe and the radiation panel of a spacecraft [1, 2]. The introduction of such elements into the model presents no great problems and can be carried out with the use of the techniques of [2]. As the investigations carried out show, the presence of certain thermal resistances on the portions of energy supply to the casing of the heat pipe and the portion of energy removal virtually has no effect on the operating parameters of the heat pipe directly but leads only to an increase in the temperature gradients over the radial coordinate on these portions and accordingly to a certain increase in the temperature of the cooled element as compared to the version where the thermal resistances between elements are minimum or entirely absent.

CONCLUSIONS

1. We have formulated a model of heat and mass transfer in low-temperature heat pipes that describes the hydrodynamic and thermal processes in the vapor phase within the framework of the boundary-layer model and the hydrodynamic processes in the liquid phase of a cooling agent within the framework of Darcy's model.

2. The distributions of the hydrodynamic and thermodynamic parameters found from solution of the problem are, on the whole, in satisfactory agreement with the existing experimental data [2, 10] and the results of theoretical investigations [3, 4].

3. The data obtained can be used in analyzing the efficiency and power of low-temperature heat pipes.

NOTATION

T_1, temperature of the casing of the heat pipe, K; r, transverse coordinate, m; z, longitudinal coordinate, m; λ_1, thermal conductivity of the aluminum casing of the heat pipe, W/(m·K); δ_2, radius of the heat pipe, m; q, specific density of the heat flux, W/m^2; L_1, length of the evaporation zone, m; L_2, length of the condensation zone, m; L, length of the heat pipe, m; ε, reduced emissivity factor; T_{surf}, surface temperature, K; δ_1, internal radius of the pipe, m; T_2, temperature of the liquid, K; P_2, pressure of the liquid, Pa; P_3, pressure of the vapor, Pa; σ, surface tension, N/m; R_{curv}, radius of curvature of the surface, m; u_2, longitudinal component of the velocity in the liquid phase, m/sec; K, permeability, m^2; μ_2, dynamic viscosity of NH_3 (liquid phase), N·sec/m^2; ε_1, porosity; C_2, heat capacity of NH_3 (liquid phase), J/(kg·K); ρ_2, density of NH_3 (vapor phase), kg/m^2; ε_1, thermal conductivity of NH_3 (liquid phase), W/(m·K); δ, radius of the vapor channel, m; λ_3, thermal conductivity of NH_3 (vapor phase), W/(m·K); T_3, temperature of the vapor, K; W_1, mass velocity of evaporation, kg/(m^2·sec); Q, heat of phase transition, J/kg; W_2, mass velocity of condensation, kg/(m^2·sec); $T_{ph.b}$, temperature at the phase boundary, K; ρ_3, density of NH_3 (vapor phase), kg/m^3; u_3, longitudinal component of the velocity in the vapor phase, m/sec; v_3, radial component of the velocity in the vapor phase, m/sec; C_3, heat capacity of NH_3 (vapor phase), J/(kg·K); M, molecular weight, kg/mole; R_1, gas constant, J/(mole·K); σ_1, Stefan–Boltzmann constant, J/K; A, accommodation coefficient; P^{sat}, saturated-vapor pressure, Pa; P, partial pressure, Pa; ε^*, small positive number. Subscripts and superscripts: surf, surface; curv, curvature; ph.b, phase boundary; sat, saturated.

REFERENCES

1. V. G. Voronin, A. V. Revyakin, and V. Ya. Sasin, *Low-Temperature Heat Pipes for Aircraft* [in Russian], Moscow (1976).
2. L. L. Vasil'ev, *Low-Temperature Pipes and Porous Heat Exchangers* [in Russian], Minsk (1977).
3. P. I. Bystrov, A. I. Ivlyutin, and A. N. Shul'ts, *Inzh.-Fiz. Zh.*, **60**, No. 2, 211–217 (1991).

4. M. M. Levitan and T. L. Perel'man, *Zh. Tekh. Fiz.*, **44**, No. 8, 1569–1591 (1974).
5. V. M. Paskonov, V. I. Polezhaev, and L. A. Chudov, *Numerical Modeling of Heat and Mass Transfer Processes* [in Russian], Moscow (1984).
6. A. A. Samarskii, *Introduction to the Theory of Difference Schemes* [in Russian], Moscow (1987).
7. R. C. Reid, J. Prausnitz, and T. K. Sherwood, *The Properties of Gases and Liquids* [Russian translation], Leningrad (1982).
8. G. N. Dul'nev and V. G. Parfenov, *Use of Computers for Solving Heat Transfer Problems* [in Russian], Moscow (1990).
9. *Handbook of Thermal Physics* [in Russian], Moscow (1976).
10. M. G. Semena, A. G. Kostornov, and A. N. Gershuni, *Inzh.-Fiz. Zh.*, **31**, No. 3, 449–455 (1976).